Semi-Quantitative [18F]FDG-PET/CT ROC-Analysis-Based Cut-Offs for Aortitis Definition in Giant Cell Arteritis

Olivier Espitia, Jérémy Schanus, Christian Agard, Françoise Kraeber-Bodéré, Alexis F Guédon, Antoine Bénichou, Jean-Michel Serfaty, Sandrine Coudol, Matilde Karakachoff, Bastien Jamet

▶ **To cite this version:**

Olivier Espitia, Jérémy Schanus, Christian Agard, Françoise Kraeber-Bodéré, Alexis F Guédon, et al.. Semi-Quantitative [18F]FDG-PET/CT ROC-Analysis-Based Cut-Offs for Aortitis Definition in Giant Cell Arteritis. International Journal of Molecular Sciences, 2022, 23 (24), pp.15528. 10.3390/ijms232415528 . hal-04743216

HAL Id: hal-04743216
https://hal.science/hal-04743216v1

Submitted on 18 Oct 2024

HAL is a multi-disciplinary open access archive for the deposit and dissemination of scientific research documents, whether they are published or not. The documents may come from teaching and research institutions in France or abroad, or from public or private research centers.

L'archive ouverte pluridisciplinaire **HAL**, est destinée au dépôt et à la diffusion de documents scientifiques de niveau recherche, publiés ou non, émanant des établissements d'enseignement et de recherche français ou étrangers, des laboratoires publics ou privés.

Distributed under a Creative Commons Attribution 4.0 International License

International Journal of
Molecular Sciences

MDPI

Article

Semi-Quantitative [^{18}F]FDG-PET/CT ROC-Analysis-Based Cut-Offs for Aortitis Definition in Giant Cell Arteritis

Olivier Espitia [1,*], Jérémy Schanus [1], Christian Agard [1], Françoise Kraeber-Bodéré [2], Alexis F. Guédon [1], Antoine Bénichou [1], Jean-Michel Serfaty [3], Sandrine Coudol [4], Matilde Karakachoff [4] and Bastien Jamet [2]

1 Department of Internal and Vascular Medicine, CHU Nantes, Nantes Université, F-44000 Nantes, France
2 Department of Nuclear Medicine, CHU Nantes, Nantes Université, CNRS, INSERM, CRCINA, F-44000 Nantes, France
3 Department of Cardiovascular Imaging, CHU Nantes, Nantes Université, F-44000 Nantes, France
4 Pôle Hospitalo-Universitaire 11, Santé Publique, Clinique des Données, CHU Nantes, Nantes Université, INSERM, CIC 1413, F-44000 Nantes, France
* Correspondence: olivier.espitia@chu-nantes.fr; Tel.: +33-240-083-355; Fax: +33-240-083-379

Abstract: [^{18}F]fluorodeoxyglucose-positron emission tomography/computed tomography ([^{18}F]FDG-PET/CT) is used to diagnose large vessel vasculitis in giant cell arteritis (GCA). We aimed to define a semi-quantitative threshold for identifying GCA aortitis from aortic atheroma or the control. Contrast enhanced computed tomography (CECT) was used as the reference imaging for aortic evaluation and to define aortitis, aortic atheroma and control aortas. [^{18}F]FDG-PET/CT was performed on 35 GCA patients and in two different control groups (aortic atheroma (n = 70) and normal control (n = 35)). Aortic semi-quantitative features were compared between the three groups. GCA patients without aortitis on CECT were excluded. Of the GCA patients, 19 (54.3%) were not on glucocorticoids (GC) prior to [^{18}F]FDG-PET/CT. The SUV_{max}, TBR_{blood} and TBR_{liver} aortic values were significantly higher in the GCA aortitis group than in the aortic atheroma and control groups ($p < 0.001$). Receiver operating characteristic curve analyses brought to light quantitative cut-off values allowing GCA aortitis diagnosis with optimal sensitivity and specificity versus control or aortic atheroma patients for each PET-based feature analyzed. Considering the overall aorta, a SUV_{max} threshold of 3.25 and a TBR_{blood} threshold of 1.75 had a specificity of 83% and 75%, respectively, a sensitivity of 81% and 81%, respectively, and the area under the ROC curve (AUC) was 0.86 and 0.83, respectively, for aortitis detection compared to control groups in GCA cases with GC. A SUV_{max} threshold of 3.45 and a TBR_{blood} threshold of 1.97 had a specificity of 90% and 93%, respectively, a sensitivity of 89% and 89%, respectively, with an AUC of 0.89 and 0.96, respectively, for aortitis detection compared to the control in GC-free GCA cases. Discriminative thresholds of SUV_{max} and TBR_{blood} for the diagnosis of GCA aortitis were established using CECT as the reference imaging.

Keywords: [^{18}F]FDG-PET/CT; aortitis; giant cell arteritis; aortic atheroma; large vessel vasculitis; diagnostic semi-quantitative thresholds

check for updates

Citation: Espitia, O.; Schanus, J.; Agard, C.; Kraeber-Bodéré, F.; Guédon, A.F.; Bénichou, A.; Serfaty, J.-M.; Coudol, S.; Karakachoff, M.; Jamet, B. Semi-Quantitative [^{18}F]FDG-PET/CT ROC-Analysis-Based Cut-Offs for Aortitis Definition in Giant Cell Arteritis. *Int. J. Mol. Sci.* **2022**, *23*, 15528. https://doi.org/10.3390/ijms232415528

Academic Editor: Hajime Kono

Received: 11 October 2022
Accepted: 5 December 2022
Published: 8 December 2022

Publisher's Note: MDPI stays neutral with regard to jurisdictional claims in published maps and institutional affiliations.

Copyright: © 2022 by the authors. Licensee MDPI, Basel, Switzerland. This article is an open access article distributed under the terms and conditions of the Creative Commons Attribution (CC BY) license (https://creativecommons.org/licenses/by/4.0/).

1. Introduction

Giant cell arteritis (GCA) is the most frequent primary vasculitis and affects large arteries. In GCA, two overlapping phenotypes of the vasculitis can be distinguished: cephalic and large vessel (LV) GCA [1]. At GCA diagnosis, aortitis is observed in about half of the cases [2–4]; the presence of aortitis at diagnosis is associated with more relapses or more vascular events during the course of the disease [5–7]. For LV assessment, the European League against Rheumatism (EULAR) [8] recommends performing contrast enhanced computed tomography (CECT) or [^{18}F]fluorodeoxyglucose-positron emission tomography with computed tomography ([^{18}F]FDG-PET/CT). Thus, in this population of elderly patients, where atheromatous disease is also commonly present, it is important to properly define aortitis on LV imaging.

To date, visual analysis is recommended for assessing [^{18}F]FDG-PET/CT in GCA detection using the systematic predefined liver background uptake as a diagnostic threshold (aspect of vasculitis when vascular wall uptake is superior to liver background uptake) [8,9], which depends on the expertise of the physicians and may lack precision of metrics due to visual FDG uptake categorization with the liver uptake as reference.

Alternatively, semi-quantitative diagnostic analytical approaches are more recent and scarce but seem to bring new light in [^{18}F]FDG-PET/CT GCA assessment [10–12]. To limit the reader bias, increase reproducibility and optimize precision, semi-quantitative analysis may be preferred. On the PET image, semi-quantitative methods use regions of interest (ROI) to determine maximum standard uptake values (SUV) [10]. In vasculitis, Target-to-Background Ratios (TBR), which is the ratio of the SUV of the arterial wall to the reference tissue (e.g., liver or blood pool), are also used to quantify arterial FDG uptake [13]. Guidelines for FDG-PET imaging recommend the use of TBR, normalizing to venous blood pool instead of SUV, for the quantification of arterial wall FDG uptake [9].

A few studies have already tried to identify quantitative thresholds for the diagnosis of GCA aortitis using [^{18}F]FDG-PET/CT, but the different thresholds identified were not discriminating [14–17]. Moreover, none of these studies have compared [^{18}F]FDG-PET/CT with CECT as the reference imaging, with each of them using temporal artery biopsy and clinical diagnosis as the reference method [14–16]. Using CECT as a reference is important because only 50% of GCA patients have aortitis, so we cannot analyze aortic [^{18}F]FDG uptake of all GCA patients to identify the cut-off for aortitis. In addition, CECT allows for differentiation of aortitis from aortic atheromatous plaques which are also responsible for [^{18}F]FDG uptake. Thus, the semi-quantitative method to evaluate GCA patients requires further clarification, in order to find out a semi-quantitative threshold for GCA aortitis detection.

The aim of this study was to identify semi-quantitative cut-offs derived from [^{18}F]FDG-PET/CT imaging using receiver operating characteristic (ROC) curves for identifying GCA-associated aortitis, with CECT as the reference imaging.

2. Results

2.1. Patients

Thirty-five GCA aortitis patients were matched with 70 aortic atheroma cases and 35 control patients without either atheroma or aortitis. The mean age was 68.3 (±8.8), 70.7 (±9.0) and 67.9 (±7.9) years in the GCA aortitis, aortic atheroma, and control group, respectively. In this study of GCA aortitis, as in most studies of GCA, there was a female predominance. In the aortitis group, 19 (54.3%) GCA patients were glucocorticosteroid-free before PET. The median time from initiation of corticosteroid therapy to completion of the PET was 7 days for 16 (45,7%) GCA patients with glucocorticosteroid (GC) treatment started before PET.

In both the aortic atheroma and the control group, patients had a history of neoplasia: 24 (34.3%) and 8 (22.9%) with hematologic malignancies, respectively, 21 (30.0%) and 25 (71.4%) with melanomas, respectively, 15 (21.4%) with pulmonary neoplasia and none in the control group, 5 (10.0%) with gastrointestinal cancers and none in control group and 5 (4.3%) and 2 (5.7%) with other neoplasia (breast cancer, ENT, skin squamous cell carcinoma), respectively. None of the included patients had active cancer or were undergoing chemotherapy. The characteristics of the patients are summarized in Table 1.

Table 1. Patients' clinical characteristics (GFR glomerular filtration rate; *p* value 1 GCA aortitis vs. Aortic atheroma; *p* value 2 GCA aortitis vs. control).

	GCA Aortitis *n* = 35	Aortic Atheroma *n* = 70	Control *n* = 35	*p* Value 1	*p* Value 2
Median age (Q1–Q3)	67 (60.7–72.2)	73 (63–77)	70 (61.5–74)	0.21	0.64
Female sex *n* (%)	30 (85.7)	61 (87.1)	30 (85.7)	0.84	>0.99
FDG-PET/CT parameters					
Mean ^{18}F-FDG dose (MBq/kg)	3.0 (±0.06)	3.0 (±0.05)	3.0 (±0.04)	0.09	0.17
Mean time between injection and imaging (min) (±SD)	64.8 (±6.8)	63.5 (±7.6)	62.1 (±6.3)	0.38	0.004
Biological settings					
Mean blood glucose level before FDG-PET/CT imaging (mmol/L) (±SD)	5.3 (±0.98)	5.5 (±1.0)	5.6 (±1.24)	0.34	0.43
CRP > 10 mg/L *n* (%)	22 (62.9)	8 (11.4)	3 (8.6)	<0.001	<0.001
CRP mg/L mean ± SD	65.7 ± 55.2	8.8 ± 30.4	2.7 ± 9.8	<0.001	<0.001
Glucocorticoids before PET *n* (%)	16 (45.7)	9 (12.6)	2 (5.7)	0.001	<0.001
Patients with hepatic cytolysis *n* (%)	1 (2.9)	14 (20.0)	6 (17.1)	0.02	0.04
GFR mL/min(±SD)	81.5 (±16.6)	80.2 (±20.0)	85.8 (±17.8)	0.70	0.30
GFR <60 mL/min *n* (%)	4 (11.4)	8 (11.4)	3 (8.5)	>0.99	0.69

2.2. [^{18}F]FDG-PET/CT Semi-Quantitative Features

The aortic, liver and blood SUV_{max} are presented for each group in Table 2 with an intra-aortitis group comparison with and without GC treatment.

Table 2. SUV_{max} liver, blood and highest aortic SUV_{max} according to aortitis, aortic atheroma and control groups (GCA: giant cell arteritis; GC: glucocorticosteroid).

Mean; Median [IQR]	GCA Aortitis without GC *n* = 19	GCA Aortitis Treated with GC *n* = 16	Aortic Atheroma *n* = 70	Control *n* = 35	*p*
SUV_{max} liver	3.3;3.2 [2.95, 3.40]	3.4;3.4 [3.08, 3.52]	3.3;3.2 [2.95, 3.60]	3.6;3.4 [3.20, 3.90]	0.047
SUV_{max} blood	1.8;1.9 [1.50, 1.95]	1.8;1.9 [1.58, 2.02]	1.8;1.8 [1.60, 2.00]	1.9;1.8 [1.60, 2.10]	0.697
SUV_{max} aortic	5.9;5.5 [4.25, 7.40]	4.1;3.9 [3.38, 4.53]	2.9;2.90 [2.65, 3.20]	2.9;2.9 [2.70, 3.00]	<0.001
TBR liver	1.8;1.6 [1.31, 2.35]	1.2;1.1 [0.97, 1.45]	0.8;0.8 [0.73, 0.88]	0.9;0.9 [0.82, 0.97]	<0.001
TBR blood	3.4;3.0 [2.33, 4.21]	2.3;2.1 [1.84, 2.76]	1.6;1.5 [1.39, 1.77]	1.7;1.6 [1.49, 1.81]	<0.001

Table 3 shows SUV_{max}, TBR_{liver} and TBR_{blood} according to aortic FDG uptake visual grading.

Table 3. Semi-quantitative aortic FDG uptake according to the visual grade of FDG uptake.

Aortic Visual Grading	SUV_{max}	TBR_{liver}	TBR_{blood}
Grade 0	2.6 ± 0.4	0.8 ± 0.1	1.4 ± 0.3
Grade 1	2.8 ± 0.5	0.9 ± 0.1	1.6 ± 0.3
Grade 2	3.6 ± 0.5	1.0 ± 0.2	1.9 ± 0.4
Grade 3	5.1 ± 1.7	1.6 ± 0.5	2.9 ± 1.2

In the overall aortic analysis as well as for each of the five aortic segments, all the SUV_{max}, TBR_{blood} and TBR_{liver} values were significantly higher in the GCA aortitis group than in the aortic atheroma and control groups (Figure 1 and Supplemental Figures S1 and S2).

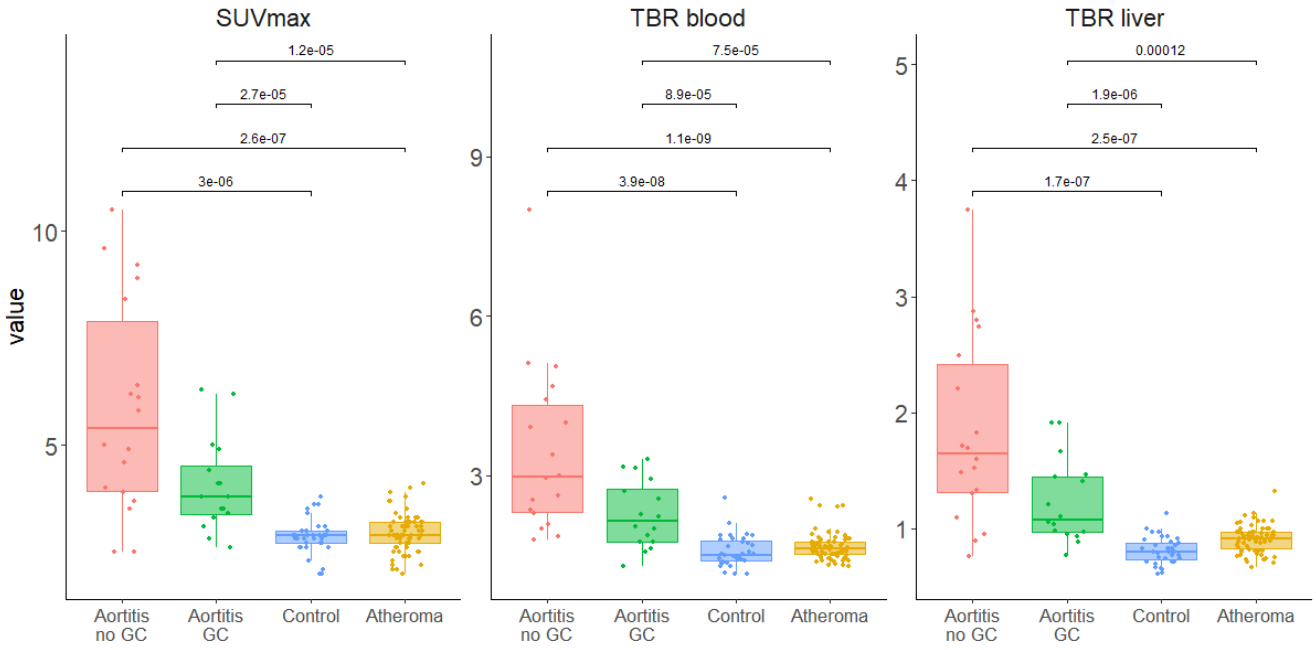

Figure 1. SUV_{max}, TBR_{blood} and TBR_{liver} aortic values in an overall aorta analysis in aortitis, aortic atheroma and control groups (GC: glucocorticosteroid).

2.3. Diagnostic Semi-Quantitative Cut-Off Values from ROC Curves

Analysis has shown that the following parameters, SUV_{max} and TBR_{blood}, provide the best discrimination between arteritis, atheroma and controls and these will be presented in detail. With regard to the ROC curves, comparisons of the different PET values between aortitis versus aortic atheroma and aortitis versus control found excellent AUCs for each [^{18}F]FDG-PET/CT-derived semi-quantitative feature analyzed (SUV_{max}, TBR_{blood} and TBR_{liver}, Supplemental Figures S3–S6). For all of them, clear diagnostic cut-off values were defined with excellent specificities and sensitivities (Table 4, Figure 2 and Supplemental Tables S1–S3).

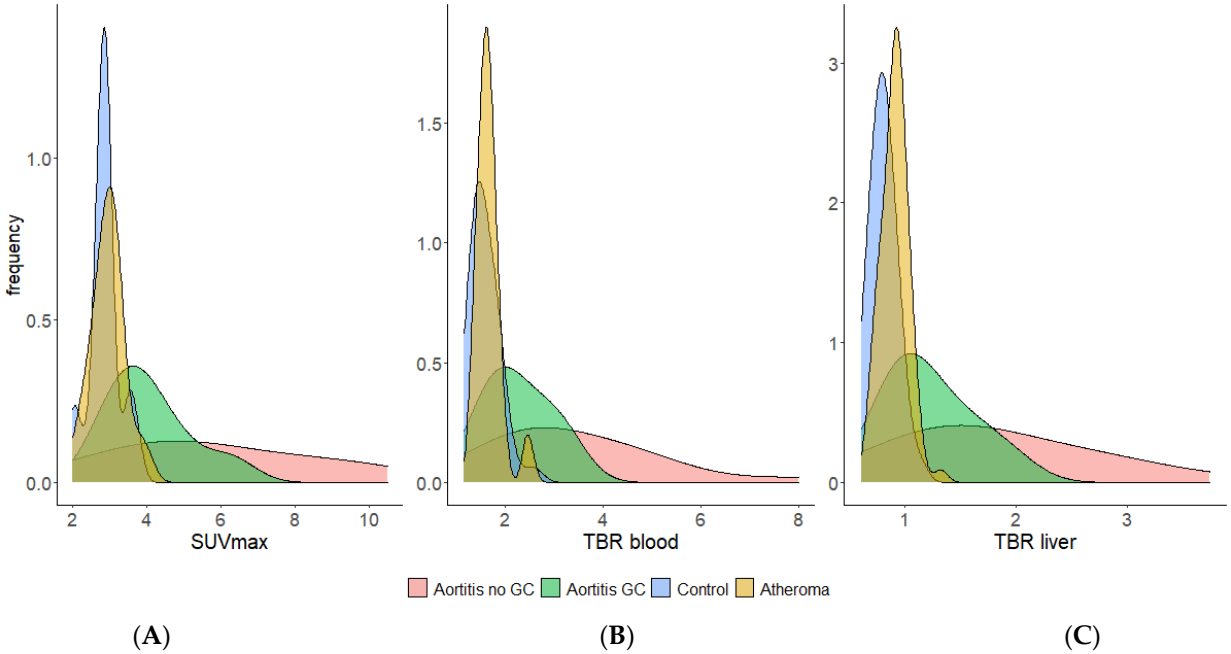

Figure 2. Frequency (density) distribution of SUV_{max} (**A**), TBR_{blood} (**B**) and TBR_{liver} (**C**) values of overall aorta in aortitis, aortic atheroma and control groups.

Specific thresholds were identified for each of the aortic segments by comparing patients with CGA aortitis without GC versus normal controls or atheromatous patients (Supplemental Tables S1–S3). When comparing patients with GCA aortitis who had GC before the PET with normal controls and atheromatous patients, in an overall aortic analysis, the AUC was 0.86 and a threshold SUV_{max} of 3.25 had a sensitivity of 81% and a specificity of 83% compared with all control patients. For GCA-aortitis without GC before PET vs. all controls, the AUC was 0.89 and a threshold SUV_{max} of 3.45 had a sensitivity of 89% and a specificity of 90% (Table 4).

Table 4. Aortic PET values in aortitis with glucocorticosteroid vs. all control patients (aortic atheroma patients and normal aortic control patients) receiver operating characteristic (ROC) curve analyses, and aortitis without glucocorticosteroid vs. all control patients ROC curve analyses in thoracic and abdominal aorta and in overall aorta (AUC: area under the curve, GC: glucocorticoids, CI: confidence interval).

	Aortitis with GC vs. All Controls			**Aortitis without GC vs. All Controls**		
	SUV_{max}	**TBR Blood**	**TBR Liver**	**SUV_{max}**	**TBR Blood**	**TBR Liver**
			Overall aorta			
AUC [CI 95%]	0.86 [0.74;0.98]	0.83 [0.69;0.96]	0.85 [0.73;0.96]	0.89 [0.76;1]	0.96 [0.93;1]	0.91 [0.81;1]
Cut-off	3.25	1.75	0.97	3.45	1.97	1.09
Specificity	0.83	0.75	0.82	0.90	0.93	0.96
Sensitivity	0.81	0.81	0.75	0.89	0.89	0.83
			Thoracic aorta			
AUC [CI 95%]	0.89 [0.79;0.99]	0.84 [0.73;0.96]	0.89 [0.79;0.98]	0.90 [0.78;1]	0.96 [0.93;1]	0.93 [0.84;1]
Cut-off	3.25	1.75	0.97	3.45	1.77	1.09
Specificity	0.81	0.80	0.80	0.93	0.81	0.97
Sensitivity	0.88	0.81	0.88	0.88	1	0.82
			Abdominal aorta			
AUC [CI 95%]	0.89 [0.79;0.98]	0.93 [0.86;1]	0.89 [0.80;0.98]	0.90 [0.78;1]	0.94 [0.86;1]	0.94 [0.85;1]
Cut-off	3.05	1.5	0.91	3.95	1.81	1.13
Specificity	0.76	0.71	0.73	0.99	0.96	1
Sensitivity	0.91	1	0.91	0.75	0.88	0.88

3. Discussion

This study is the first to put forward accurate PET-derived semi-quantitative thresholds values for GCA aortitis detection using CECT as reference. In addition, the vascular [^{18}F]FDG uptake of GCA patients was compared with two different control groups, including an aortic atheroma group, using the same methods. In GCA cases without and with GC before PET/CT, specific aortic cut-off values allowing aortitis to be distinguished from atheromatous lesions, as well as from normal aortic uptake, with a very good sensitivity and specificity have been identified for SUV_{max}, TBR_{blood} and TBR_{liver}.

Currently, the analysis of aortic [^{18}F]FDG uptake is performed visually in comparison to hepatic [^{18}F]FDG uptake. This study showed that liver and aortitis SUV were close. Thus, a semi-quantitative analysis, with identification of discriminatory cut-offs values, could be an aid to interpretation and could improve the reproducibility of the analyses. It could be complementary to qualitative analysis and could be useful to automate interpretation; although, the presence of grade 3 [^{18}F]FDG uptake of all segments of the aorta and extensive involvement of the supra-aortic trunks and lower limbs are also important diagnostic features of aortitis [10].

Semi-quantitative analysis compared to qualitative analytical approaches could limit the reader bias, increase reproducibility, and optimize precision. Qualitative assessment may be less reliable and accurate compared to semi-quantitative approaches, especially SUV_{max} and TBR_{blood}. In addition, SUV_{max} and TBR_{blood} are not yet routinely and easily used PET-based features so our findings are clinically relevant.

Glomerular filtration rate (GFR) can also affect PET-derived features, especially TBR_{blood}. Indeed, it has been shown that GFR is negatively associated with FDG distribution in the blood pool [13]. Rosenblum et al. showed that at one-hour imaging the three factors most strongly associated with [^{18}F]FDG blood pool background uptake were uptake time, GFR and body mass index [13]. Moreover, in 2014, Besson et al. reported in a semi-quantitative approach to biopsy proven GCA that the aortic to venous blood pool SUV_{max} ratio outperformed the lung and liver ratios [14]. Thus, features involving SUV blood pool could be of interest for aortitis analysis.

In this study, AUC from SUV_{max}, TBR_{blood} or TBR_{liver} were high compared to previous studies [15]. This could be explained by the fact that, in this study, every patient had aortitis diagnosed on CT, unlike previous studies which included patients with GCA but without aortic reference imaging (other than PET/CT). However, according to the literature, 50% of GCA patients do not have aortitis at the time of GCA diagnosis, so these previous studies included a number of GCA patients without aortitis, thus lowering the AUC and the SUV_{max}.

It is difficult then to determine the best method for PET analysis of large vessel vasculitis in GCA. Qualitative visual assessment requires physician experience and is subjective. Visual PETVAS scoring is more strongly associated with physician interpretation of PET activity rather than TBR or SUV metrics. TBRs outperformed SUV metrics in vascular inflammation in large-vessel vasculitis [11]. The continuous scale of semi-quantitative scoring systems leads to a better ability to discriminate change in PET activity across a wider range of values [11]. Therefore, we propose to mix visual and semi-quantitative analysis in [^{18}F]FDG-PET/CT large vessel vasculitis reports.

This study has several limitations, such as its retrospective design, the number of patients included and the maximum interval of 10 days between the start of corticosteroid therapy and [^{18}F]FDG-PET/CT imaging. [^{18}F]FDG uptake and, consequently, the test's sensitivity, decreases significantly after GC exposure [18]. In our study, more than one third of GCA patients underwent [^{18}F]FDG-PET/CT imaging after the start of steroid therapy. Thus, as in the study by Nielsen et al. [18], we observe a decrease in aortic SUV_{max}, TBR_{liver} and TBR_{blood}. However, in our study the GCA patients were different as they were included with inflammatory thickenings of the aortic wall on CECT; thus, these structural wall remodelings could favor the persistence of FDG uptake despite more than 3 days of GC treatment. However, in daily practice, the start of GC therapy is often urgent because of the risk of visual impairment, and cannot wait for the PET/CT imaging. Thus, these data seem appropriate for the management of these patients.

Moreover, [^{18}F]FDG-PET/CT imaging were performed with analogical devices, thus the results of the semi-quantitative diagnostic cut-off values might be slightly different with a new generation of digital PET/CT devices. Indeed, these new devices offer better spatial resolution reducing the partial volume effect and could improve [^{18}F]FDG uptake values. Therefore, the semi-quantitative diagnostic cut-off values found in this work need to be further supported in studies relying on digital PET/CT devices.

The results of this exploratory study need to be confirmed by prospective and multicenter evaluation performed on multiple PET/CT devices.

In conclusion, this study identified discriminative diagnostic cut-off values for different semi-quantitative [^{18}F]FDG-PET/CT-derived parameters. These results rely on a CECT reference test which defines aortitis or atheroma. Beyond visual analysis, PET advanced understanding using SUV_{max} and TBR thresholds values could be used for the accurate diagnosis of GCA aortitis. If these results are validated in prospective and multicenter studies, they could be useful for the diagnosis of aortitis with the development of artificial intelligence for the analysis of aortic walls. Thus, SUV_{max} cut-offs of 3.25 and 3.45 could be used to identify GCA aortitis in patients with and without GC before PET.

The use of SUV blood pool values to normalize the interpretation seems interesting since SUV blood is less influenced by corticosteroid therapy than SUV liver. In this way, TBR_{blood}, with cut-off values between 1.75 and 1.97 in GCA patients with and without

GC before PET, seems to be a good parameter for the analysis of aortic disease with a good AUC, specificity and sensitivity. Multicenter studies are needed to validate these discriminative PET thresholds.

4. Materials and Methods

4.1. Standard Reference

We used CECT as the reference imaging to analyze the aortic wall. We defined three categories of aortic wall: wall with aortitis, wall with atheroma and normal aortic wall (Figure 3).

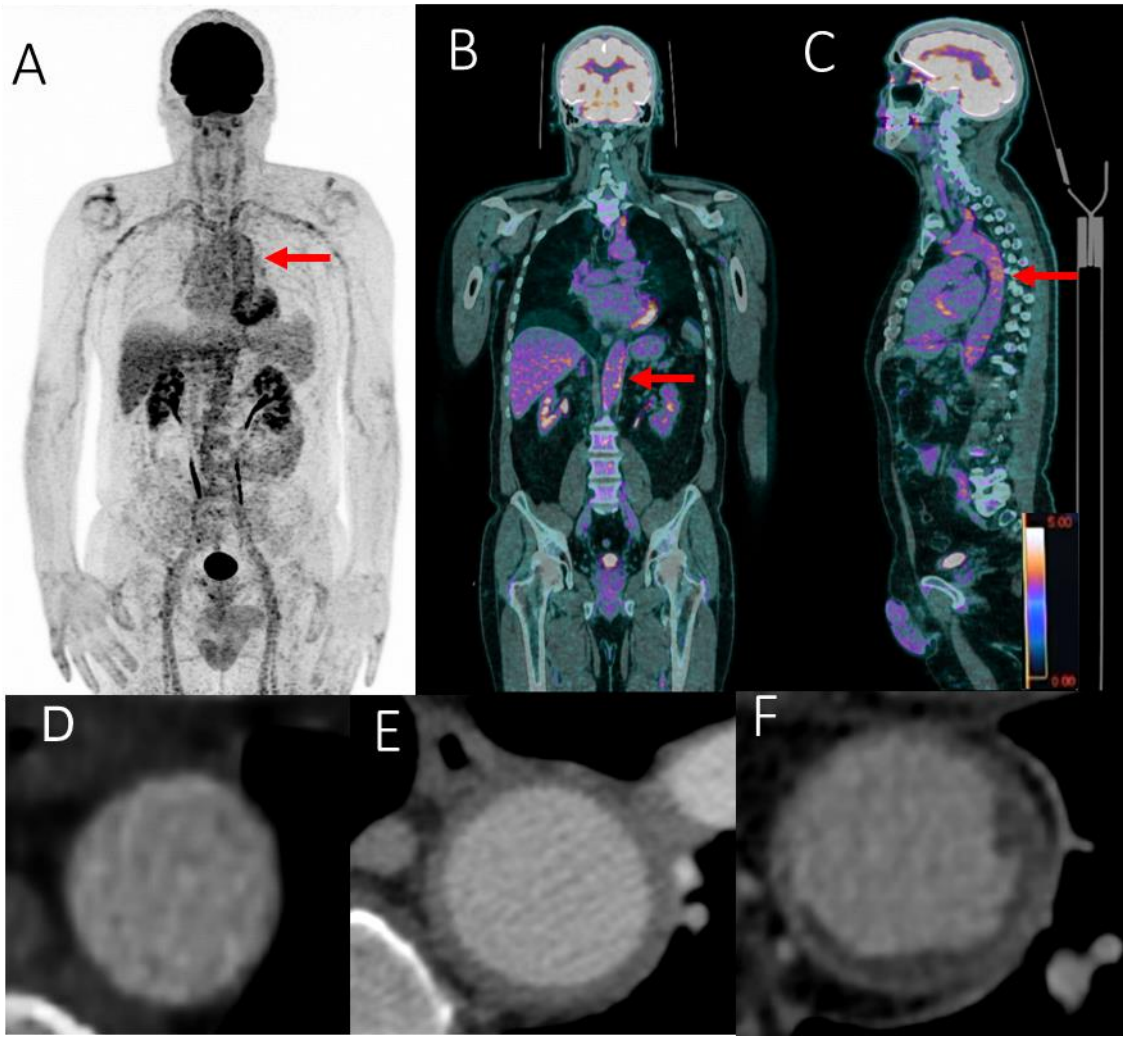

Figure 3. FDG-PET/CT showing grade 3 (red arrows) scattered large vessel vasculitis uptake (including the thoracic and abdominal aorta) in maximum intensity projection (MIP) image (**A**), including the abdominal (**B**) and thoracic aorta (**C**) in coronal and sagittal fused (PET with CT) slices. SUVmax value in the abdominal aortic wall: 6.45. Aortic evaluation with contrast enhanced computed tomography: normal aorta (**D**), aortitis (**E**) and aortic atheroma (**F**).

This monocentric retrospective study included patients diagnosed with aortitis related to GCA between June 2014 and June 2021. Each GCA case included in this study underwent a CECT and [^{18}F]FDG-PET/CT before starting corticosteroid therapy, or within no more than 10 days after its initiation [10].

All GCA patients had to meet at least three American College of Rheumatology (ACR) criteria for the diagnosis of GCA [19], or be over 50 years of age with C-reactive Protein (CRP) $\geq$ 10 mg/L and large vessel vasculitis.

Aortitis was defined by CECT with a circumferential aortic parietal thickening > 2.2 mm [20] (Figure 3).

Each GCA-related aortitis patient was matched with two aortic atheroma control cases proven on CECT and with one control patient without aortic atheroma (Figure 3). Matching was done on both sex and age. Aortic atheroma control cases had to have at least two out of five CT-positive aortic segments to be included in the study as previously described [10]. The aortic atheromatous patients and control patients were drawn from a group of patients with a history of neoplasia both followed with [^{18}F]FDG-PET/CT and CECT.

Aortic atheroma was defined by CECT as an atheromatous lesion with a semi-quantitative ranging $\geq$1 (score ranging from 0 to 2: 0 for the absence of plaque; 1 for the presence of smooth thin plaques and 2 for the presence of thick irregular plaques ($\geq$3 mm)) [20].

All aortic atheromatous patients and control cases were free of neoplasia at the time of assessment and had not received oncology treatment for at least 3 months. Patients with active cancer or who had been treated within 3 months were excluded.

4.2. [^{18}F]FDG-PET/CT Acquisition and Analysis

For the PET acquisition method, after at least 6 h of fasting, 3 MBq/kg of [^{18}F]FDG was injected intravenously (after recording baseline blood glucose level). After 60 min of resting, [^{18}F]FDG-PET/CT imaging was recorded in a supine position from the skull to the base of the thighs with arms next to the body. Images were acquired on a Siemens Biograph mCT64. First, non-contrast CT acquisition was performed with a multi-slice spiral CT scan (Figure 3). Blood glucose levels were measured before [^{18}F]FDG injection with a preferred glycemia level $\leq$ 150 mg/dL; however, up to 200 mg/dL was allowed. Next, a PET acquisition of the same axial range was performed with the patient in the same position. PET data were reconstructed using the Ordinary-Poisson OSEM provided by the manufacturer. All data were corrected for attenuation, scatter and random coincidences. The reconstruction parameters were 3 iterations, 21 subsets and a Gaussian post-filtering of 2 mm FWHM. The voxel size used was 4 $\times$ 4 $\times$ 2 mm. The time per bed step was adapted following a methodology we previously published [21].

Patients who had focal instead of diffuse [^{18}F]FDG uptake in the liver were excluded.

[^{18}F]FDG-PET/CT was analyzed using a double blind centralized method; aortic images were segmented according to five anatomical regions: ascending thoracic aorta, aortic arch, descending thoracic aorta, abdominal suprarenal and infrarenal aorta.

An analysis of the different aortic segments was performed by placing Regions of Interest (ROIs) around the vessel in a cross-section. The selected segments were defined according to the Most Diseased Segment (MDS) [22], visually identified, meaning that the slice with the highest standardized uptake value (SUV_{max}) was selected, and then the mean of the SUV_{max} from this and the two neighboring slices was calculated.

Different target to background ratios (TBRs) were also recorded by measuring the SUV_{max} of each reference organ. Ratios between aortic wall SUV_{max} and reference site SUV_{max} were evaluated by placing ROIs of similar size (1 cm^3) (Figure 4):

- Target-to-liver ratio (TBR_{liver}) by placing a ROI in the healthy right lobe of the liver;
- Target-to-blood pool ratio (TBR_{blood}) defined for supra-diaphragmatic vessels by a ROI drawn centrally in the blood pool of the superior vena cava and for infra-diaphragmatic vessels in the blood pool of the inferior vena cava.

Each of these parameters were compared between the aortitis and control groups and between aortitis and aortic atheroma cases.

Next, an overall aortic analysis was performed by including only the highest values of the five segments per patient. This grouping was done for each PET-based feature. A thoracic aortic analysis was performed by grouping the three thoracic segments, and an abdominal aortic analysis was performed by grouping the two abdominal aortic segments using the same methodology.

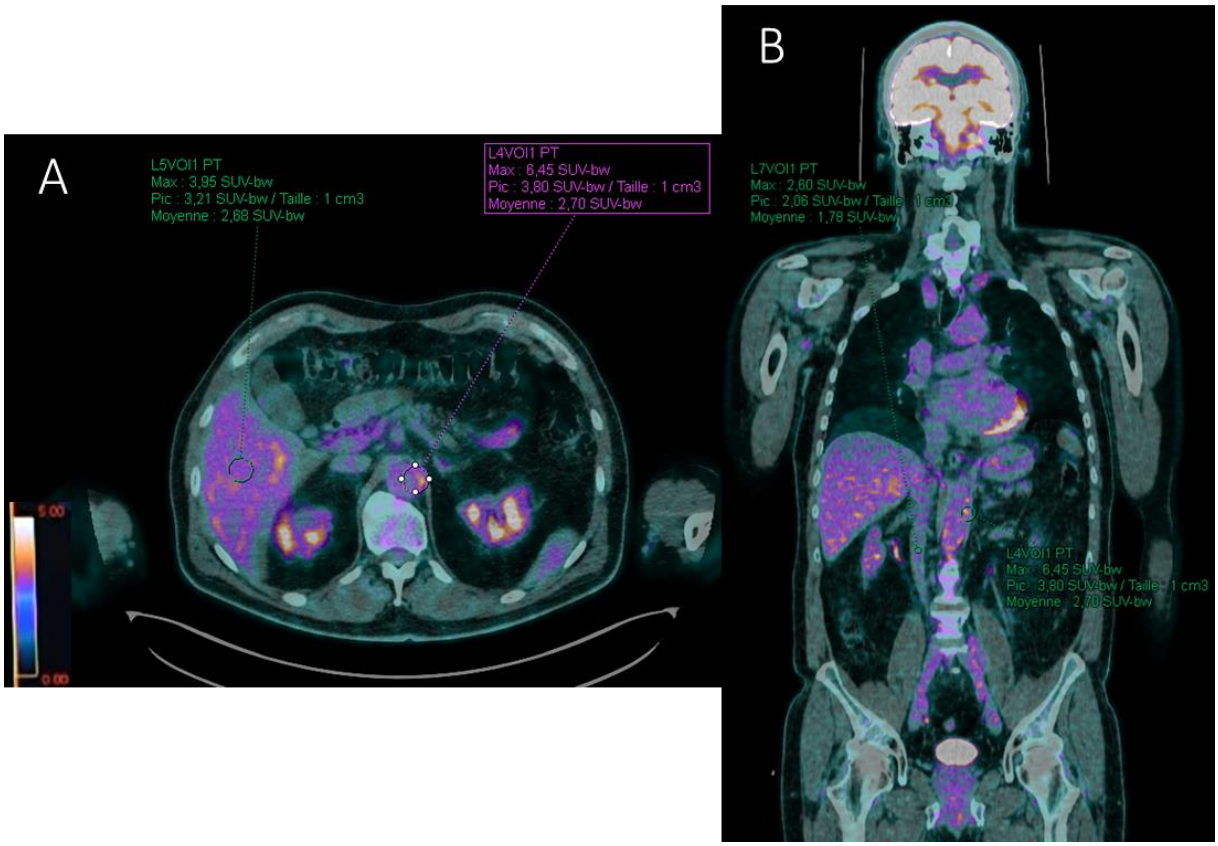

Figure 4. FDG-PET/CT axial (**A**) and coronal (**B**) fused (PET with CT) slices illustrating the computation of the target-to-liver (TBR_{liver}) and target-to-blood (TBR_{blood}) background ratios in a patient with aortitis. SUV_{max} value of the target (abdominal aortic wall) is recorded with a region of interest (ROI) drawn manually around the arterial structure. Liver (**A**) and blood pool (**B**) background SUV_{max} values are estimated with ROIs projected on the healthy right lobe of the liver and the inferior vena cava, respectively. Here, TBR_{liver} = 6.45/3.95 = 1.63 and TBR_{blood} = 6.45/2.6 = 2.48 for the abdominal aorta.

4.3. Statistical Analysis

Categorical variables were expressed in terms of counts and percentages, and quantitative variables were presented as means ± standard deviations (SD) or medians and inter-quartile range (IQR). The quantitative comparisons were assessed using a student's t-test or Wilcoxon's signed rank test in case of variables not normally distributed (assessed by Shapiro–Wilk test). Frequency comparisons were performed using Chi2 or Fisher's exact test according to the statistical headcount. For all statistical analyses, a two-tailed $p < 0.05$ was considered significant.

For overall thoracic and abdominal aortic analyses, the highest SUV_{max}, TBR_{blood} or TBR_{liver} value of the different aortic segments was chosen to perform the analysis.

Area under the ROC curve (AUC) along with a 95% confidence interval (CI) was utilized as a combined measure of sensitivity and specificity to evaluate the performance of each quantitative parameter in PET vs. control or vs. aortic atheroma. AUC values lay between 0 and 1. Metrics with capability to distinguish between binary outcomes will result in an AUC above 0.5, with larger AUC values suggesting better diagnostic performance. The Youden's J statistic was used to determine the optimal cut-off score that maximized the distance to the identity line. To simplify the visual comparison of ROC curves and diagnostic performances, binomial smoothed ROC curves were produced. ROC curves were performed through pROC R package [23]. R statistical software, version 4.0.4 was used for all statistical analyses.

Supplementary Materials: The following supporting information can be downloaded at: https://www.mdpi.com/article/10.3390/ijms232415528/s1.

Author Contributions: J.S.: data collection analysis and interpretation; O.E., B.J. and M.K.: drafting of the manuscript; J.S., C.A., A.B., F.K.-B., J.-M.S., A.F.G., S.C., O.E.: data collection and critical review; O.E., M.K. and B.J.: methodology, analysis and interpretation of data; O.E.: study concept and design, data collection, analysis and interpretation, drafting of the manuscript and supervision. All authors have read and agreed to the published version of the manuscript.

Funding: The authors declare that no funds, grants, or other support were received during the preparation of this manuscript.

Institutional Review Board Statement: This study received ethics approval by the local board of ethics of the Nantes University Hospital. Each patient included in this study received written information and informed consent was obtained from all the participants. This research study was in accordance with the Declaration of Helsinki (number: 2020-02-19, MR-003).

Informed Consent Statement: Informed consent was obtained from all subjects involved in the study.

Data Availability Statement: The data is available upon request from the corresponding author.

Conflicts of Interest: The authors declare no conflict of interest.

References

1. Gribbons, K.B.; Ponte, C.; Carette, S.; Craven, A.; Cuthbertson, D.; Hoffman, G.S.; Khalidi, N.A.; Koening, C.L.; Langford, C.A.; Maksimowicz-McKinnon, K.; et al. Patterns of Arterial Disease in Takayasu Arteritis and Giant Cell Arteritis. *Arthritis Care Res.* **2020**, *72*, 1615–1624. [CrossRef] [PubMed]
2. Blockmans, D. The Use of (18F)Fluoro-Deoxyglucose Positron Emission Tomography in the Assessment of Large Vessel Vasculitis. *Clin. Exp. Rheumatol.* **2003**, *21*, S15–S22. [PubMed]
3. Agard, C.; Barrier, J.-H.; Dupas, B.; Ponge, T.; Mahr, A.; Fradet, G.; Chevalet, P.; Masseau, A.; Batard, E.; Pottier, P.; et al. Aortic Involvement in Recent-Onset Giant Cell (Temporal) Arteritis: A Case-Control Prospective Study Using Helical Aortic Computed Tomodensitometric Scan. *Arthritis Rheum.* **2008**, *59*, 670–676. [CrossRef] [PubMed]
4. Prieto-González, S.; Arguis, P.; García-Martínez, A.; Espígol-Frigolé, G.; Tavera-Bahillo, I.; Butjosa, M.; Sánchez, M.; Hernández-Rodríguez, J.; Grau, J.M.; Cid, M.C. Large Vessel Involvement in Biopsy-Proven Giant Cell Arteritis: Prospective Study in 40 Newly Diagnosed Patients Using CT Angiography. *Ann. Rheum. Dis.* **2012**, *71*, 1170–1176. [CrossRef] [PubMed]
5. de Mornac, D.; Espitia, O.; Néel, A.; Connault, J.; Masseau, A.; Espitia-Thibault, A.; Artifoni, M.; Achille, A.; Wahbi, A.; Lacou, M.; et al. Large-Vessel Involvement Is Predictive of Multiple Relapses in Giant Cell Arteritis. *Ther. Adv. Musculoskelet. Dis.* **2021**, *13*, 1759720X211009029. [CrossRef] [PubMed]
6. Espitia, O.; Blonz, G.; Urbanski, G.; Landron, C.; Connault, J.; Lavigne, C.; Roblot, P.; Maillot, F.; Audemard-Verger, A.; Artifoni, M.; et al. Symptomatic Aortitis at Giant Cell Arteritis Diagnosis: A Prognostic Factor of Aortic Event. *Arthritis Res. Ther.* **2021**, *23*, 14. [CrossRef]
7. de Mornac, D.; Agard, C.; Hardouin, J.-B.; Hamidou, M.; Connault, J.; Masseau, A.; Espitia-Thibault, A.; Artifoni, M.; Ngohou, C.; Perrin, F.; et al. Risk Factors for Symptomatic Vascular Events in Giant Cell Arteritis: A Study of 254 Patients with Large-Vessel Imaging at Diagnosis. *Ther. Adv. Musculoskelet. Dis.* **2021**, *13*, 1759720X211006967. [CrossRef]
8. Dejaco, C.; Ramiro, S.; Duftner, C.; Besson, F.L.; Bley, T.A.; Blockmans, D.; Brouwer, E.; Cimmino, M.A.; Clark, E.; Dasgupta, B.; et al. EULAR Recommendations for the Use of Imaging in Large Vessel Vasculitis in Clinical Practice. *Ann. Rheum. Dis.* **2018**, *77*, 636–643. [CrossRef]
9. Slart, R.H.J.A.; Writing Group; Reviewer Group; Members of EANM Cardiovascular; Members of EANM Infection & Inflammation; Members of Committees, SNMMI Cardiovascular; Members of Council, PET Interest Group; Members of ASNC. EANM Committee Coordinator FDG-PET/CT(A) Imaging in Large Vessel Vasculitis and Polymyalgia Rheumatica: Joint Procedural Recommendation of the EANM, SNMMI, and the PET Interest Group (PIG), and Endorsed by the ASNC. *Eur. J. Nucl. Med. Mol. Imaging* **2018**, *45*, 1250–1269. [CrossRef]
10. Espitia, O.; Schanus, J.; Agard, C.; Kraeber-Bodéré, F.; Hersant, J.; Serfaty, J.-M.; Jamet, B. Specific Features to Differentiate Giant Cell Arteritis Aortitis from Aortic Atheroma Using FDG-PET/CT. *Sci. Rep.* **2021**, *11*, 17389. [CrossRef]
11. Dashora, H.R.; Rosenblum, J.S.; Quinn, K.A.; Alessi, H.; Novakovich, E.; Saboury, B.; Ahlman, M.A.; Grayson, P. Comparing Semi-Quantitative and Qualitative Methods of Vascular FDG-PET Activity Measurement in Large-Vessel Vasculitis. *J. Nucl. Med. Off. Publ. Soc. Nucl. Med.* **2022**, *63*, 280–286. [CrossRef]
12. Laffon, E.; Marthan, R. On Semi-Quantitative Methods for Assessing Vascular 18FDG-PET Activity in Large-Vessels Vasculitis. *J. Nucl. Med. Off. Publ. Soc. Nucl. Med.* **2022**, *63*, 325–326. [CrossRef]
13. Rosenblum, J.S.; Quinn, K.A.; Rimland, C.A.; Mehta, N.N.; Ahlman, M.A.; Grayson, P.C. Clinical Factors Associated with Time-Specific Distribution of 18F-Fluorodeoxyglucose in Large-Vessel Vasculitis. *Sci. Rep.* **2019**, *9*, 15180. [CrossRef] [PubMed]

14. Besson, F.L.; de Boysson, H.; Parienti, J.-J.; Bouvard, G.; Bienvenu, B.; Agostini, D. Towards an Optimal Semiquantitative Approach in Giant Cell Arteritis: An (18)F-FDG PET/CT Case-Control Study. *Eur. J. Nucl. Med. Mol. Imaging* **2014**, *41*, 155–166. [CrossRef] [PubMed]
15. Hautzel, H.; Sander, O.; Heinzel, A.; Schneider, M.; Müller, H.-W. Assessment of Large-Vessel Involvement in Giant Cell Arteritis with 18F-FDG PET: Introducing an ROC-Analysis-Based Cutoff Ratio. *J. Nucl. Med. Off. Publ. Soc. Nucl. Med.* **2008**, *49*, 1107–1113. [CrossRef]
16. Stellingwerff, M.D.; Brouwer, E.; Lensen, K.-J.D.F.; Rutgers, A.; Arends, S.; van der Geest, K.S.M.; Glaudemans, A.W.J.M.; Slart, R.H.J.A. Different Scoring Methods of FDG PET/CT in Giant Cell Arteritis: Need for Standardization. *Medicine* **2015**, *94*, e1542. [CrossRef]
17. Braun, J.; Baraliakos, X.; Fruth, M. The Role of 18F-FDG Positron Emission Tomography for the Diagnosis of Vasculitides. *Clin. Exp. Rheumatol.* **2018**, *36* (Suppl. 114), 108–114.
18. Nielsen, B.D.; Gormsen, L.C.; Hansen, I.T.; Keller, K.K.; Therkildsen, P.; Hauge, E.-M. Three Days of High-Dose Glucocorticoid Treatment Attenuates Large-Vessel 18F-FDG Uptake in Large-Vessel Giant Cell Arteritis but with a Limited Impact on Diagnostic Accuracy. *Eur. J. Nucl. Med. Mol. Imaging* **2018**, *45*, 1119–1128. [CrossRef]
19. Hunder, G.G.; Bloch, D.A.; Michel, B.A.; Stevens, M.B.; Arend, W.P.; Calabrese, L.H.; Edworthy, S.M.; Fauci, A.S.; Leavitt, R.Y.; Lie, J.T. The American College of Rheumatology 1990 Criteria for the Classification of Giant Cell Arteritis. *Arthritis Rheum.* **1990**, *33*, 1122–1128. [CrossRef]
20. Berthod, P.E.; Aho-Glélé, S.; Ornetti, P.; Chevallier, O.; Devilliers, H.; Ricolfi, F.; Bonnotte, B.; Loffroy, R.; Samson, M. CT Analysis of the Aorta in Giant-Cell Arteritis: A Case-Control Study. *Eur. Radiol.* **2018**, *28*, 3676–3684. [CrossRef]
21. Carlier, T.; Ferrer, L.; Necib, H.; Bodet-Milin, C.; Rousseau, C.; Kraeber-Bodéré, F. Clinical NECR in 18F-FDG PET Scans: Optimization of Injected Activity and Variable Acquisition Time. Relationship with SNR. *Phys. Med. Biol.* **2014**, *59*, 6417–6430. [CrossRef] [PubMed]
22. Bucerius, J.; Hyafil, F.; Verberne, H.J.; Slart, R.H.J.A.; Lindner, O.; Sciagra, R.; Agostini, D.; Übleis, C.; Gimelli, A.; Hacker, M.; et al. Position Paper of the Cardiovascular Committee of the European Association of Nuclear Medicine (EANM) on PET Imaging of Atherosclerosis. *Eur. J. Nucl. Med. Mol. Imaging* **2016**, *43*, 780–792. [CrossRef] [PubMed]
23. Robin, X.; Turck, N.; Hainard, A.; Tiberti, N.; Lisacek, F.; Sanchez, J.-C.; Müller, M. PROC: An Open-Source Package for R and S+ to Analyze and Compare ROC Curves. *BMC Bioinform.* **2011**, *12*, 77. [CrossRef] [PubMed]